



Spatial distribution and estimation of rainfall trends and erosivity in the Epitácio Pessoa reservoir catchment, Paraíba, Brazil

Richarde Marques da Silva¹ · Celso Augusto Guimarães Santos² ·
Jorge Flávio Cazé Braga da Costa Silva³ · Alexandro Medeiros Silva³ ·
Reginaldo Moura Brasil Neto⁴

Received: 7 January 2020 / Accepted: 11 April 2020 / Published online: 27 April 2020
© The Author(s) 2020, corrected publication September 2020

Abstract

The main goals of this study are to better understand the spatial and temporal variabilities in rainfall and to identify rainfall trends and erosivity for the period from 1963 to 1991 in the Epitácio Pessoa reservoir catchment, which is located in Paraíba, northeastern Brazil. This study analyzes annual rainfall trends on a regional scale by using monthly data from 13 rainfall stations. For this purpose, the nonparametric Mann–Kendall and Sen methods were used in the analysis. Descriptive statistics methods and interpolation techniques were also used for spatial–temporal analysis of the annual rainfall. A detailed statistical analysis applied to the time series of all the stations indicates that the rainfall presents substantial annual spatial–temporal variability and a negative trend (decrease) in the mean rainfall at most of the rainfall stations in the catchment during the study period. The results only showed a positive trend for the Soledade and Pocinhos stations. The distribution of positive and negative trends in the Epitácio Pessoa reservoir catchment is extremely irregular, and the changes in the study area are more significant compared to those identified in other studies.

✉ Celso Augusto Guimarães Santos
celso@ct.ufpb.br

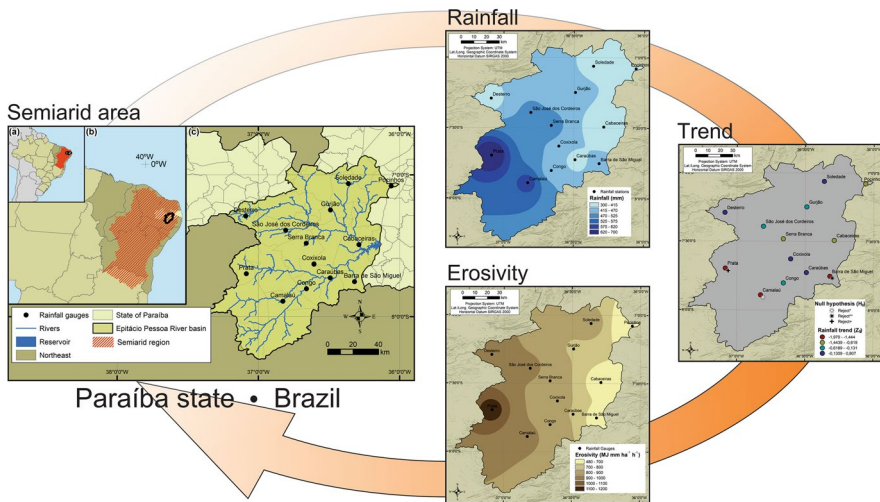
¹ Department of Geosciences, Federal University of Paraíba, João Pessoa, PB 58051-900, Brazil

² Department of Civil and Environmental Engineering, Federal University of Paraíba, João Pessoa, PB 58051-900, Brazil

³ Postgraduate Programme Geography/CCEN/UFPB, Federal University of Paraíba, João Pessoa, PB 58051-900, Brazil

⁴ Postgraduate Programme Civil and Environmental Engineering/CT/UFPB, Federal University of Paraíba, João Pessoa, PB 58051-900, Brazil

Graphic abstract



Keywords Mann–Kendall test · Rainfall variability · Sen’s test

1 Introduction

Global warming, and therefore changes in annual rainfall, has attracted the attention of researchers in different regions of the world (Mullick et al. 2019; Thomson et al. 2019; Morbidelli et al. 2018). One of the most significant consequences of global warming would be an increase or decrease in the magnitude and frequency of annual rainfall (Croitoru et al. 2013). Climate change is a very important topic and one of the main challenges at present. In addition, both the large regions of the world and the semi-arid regions need more attention.

In the past decades, climate variations have been analyzed with special attention and the results of these studies are of interest in several areas of knowledge, especially for semi-arid regions, where optimized management of water resources should be pursued and land degradation should be avoided, for example. The potential applications of this topic are numerous, including in the management of water resources and in the analysis of changes in ecosystems or in economic activities (Li et al. 2018; Moghim 2018; Guo et al. 2019). Changes in annual rainfall have been identified in several studies conducted at local, regional and global scales (Silva et al. 2015; Gocic and Trajkovic 2013; Hamlaoui-Moulai et al. 2013; Rutebuka et al. 2020).

In this study, rainfall variability is directly related to regional water management, which is of great socioeconomic and environmental importance, mainly in semi-arid regions like Paraiba State. More than 85% of the area of Paraiba State is considered semi-arid, and this state has historically suffered from constant periods of drought due to the position of the intertropical convergence zone, the El Niño–Southern oscillation and sea surface temperature, which are interrelated mechanisms that cause variability in rainfall and weather (Alves et al. 2017). The behavior of rainfall in time and space in this basin directly influences the

water volume in the reservoirs within the region; furthermore, the semiarid northeastern Brazil is one of the world's most densely populated dryland regions (Pilz et al. 2018). In addition, severe drought events might deplete the drinking water supply, as has occurred in recent continuous dry years (2012–2017).

The history of the Brazilian semiarid region, which could be considered one of the regions in the world most vulnerable to climate change (Marengo et al. 2018), is marked by droughts, water scarcity and consequently their effects, which manifest themselves in the most varied forms, such as environmental degradation, increased rural unemployment and hunger or poverty in or migration from the affected areas. Because of the irregular rainfall distribution in the region, which is below 600 mm per year in much of the region, the semiarid zone faces a chronic problem of water scarcity, which is an obstacle to the development of economic activities (Marengo 2008). Cycles of severe droughts and floods usually affect the region at intervals ranging from a few years to decades. Statistically, there are 18–20 years of drought every 100 years, which makes it difficult to analyze the variability of hydrological processes and consequently to obtain a more effective prediction of extreme events in the region (Galvão et al. 2005). In addition, estimations of future climate based on different atmospheric circulation models show that there will be global warming and an increase in climatic aridity in many zones globally. In the case of northeastern Brazil, projections predict an increase in droughts and decrease in water storage (Marengo and Bernasconi 2015; Fernandez et al. 2019).

More recently, much of Paraíba State, located in northeastern Brazil, has been experiencing one of the greatest droughts in its history (2012–2017), which directly affects the local population (Gomes et al. 2017; Santos et al. 2019a, b; Dantas et al. 2020; Alvalá et al. 2017; Marengo et al. 2018). The risks arising from climate variability, whether natural or of anthropogenic origin, have raised great concern in the scientific and political milieus, in the media and in the general population, especially in regions that are more susceptible to natural risks, such as the Brazilian semiarid region (Brito et al. 2017). There are some studies regarding the rainfall behavior trends, analysis of climate extremes and drought indices in the semiarid zone of Brazil (da Silva et al. 2016; Barbosa and Kumar 2016; Alves et al. 2017; Tomasella et al. 2018; Santos et al. 2019b; Marçal et al. 2019; Costa et al. 2020), mainly observing droughts in the last decades of the 20th century. However, none of the work provides a detailed study regarding rainfall trends, rainfall erosivity, land degradation and water management in the Epiitácio Pessoa reservoir. The Epiitácio Pessoa reservoir is a major reservoir in the semiarid region of Paraíba State that supplies 26 cities, including Campina Grande, one of the main cities in northeastern Brazil (De Medeiros et al. 2019). The annual cycle of rain and streamflow in the country varies between basins, and in fact, the interannual climate variability associated with El Niño or La Niña, or the variability in the tropical and southern Atlantic sea surface temperatures, may generate climatic anomalies that generate large droughts, such as those in the years 1877, 1983 and 1998 in northeastern Brazil (Andreoli and Kayano 2007). The droughts generated crises related to the public water supply in cities due to the constant reduction in the water stored behind dams after the beginning of the droughts (Dantas et al. 2020). As this region does not have groundwater recharge due to the crystalline basement and because it is a headwater basin, water storage depends on precipitation, which makes this basin extremely dependent on the region's drought events and the good management of water resources of the basin. In this sense, the analysis of the trend in the rainfall time series, coupled with geographic information systems, has been an important tool to identify and measure trends and to identify the existence of any deviations from trends. Thus, this study aims to identify possible trends in the rainfall time series and the erosivity in the Epiitácio Pessoa reservoir catchment.

2 Materials and methods

2.1 Characterization of the study area

The Epitácio Pessoa reservoir catchment drainage basin is located in the central portion of Paraíba State between $6^{\circ} 50' 00''$ S– $8^{\circ} 20' 00''$ S and $36^{\circ} 00' 00''$ W– $37^{\circ} 25' 00''$ W, constituting an area of 12,406 km² and a perimeter of 436 km (Fig. 1). This basin is located in the semiarid region of northeastern Brazil, more precisely on the Borborema Plateau. The Epitácio Pessoa reservoir catchment has smooth undulating relief and elevations ranging between 400 and 600 m above sea level; the mean monthly temperature is always above 26 °C (Silva et al. 2018). Its main rivers are the Upper Paraíba and the Taperoá rivers, which have intermittent flow regimes and originate in Serra do Teixeira County and Monteiro County, respectively, and terminate in the Epitácio Pessoa reservoir.

The predominant vegetation in the basin is caatinga (dry tropical forest) that presents a mosaic of different physiognomies with mostly small-sized vegetation together with cochineal cactus, cotton and agave crops (the latter two are of more commercial nature) and temporary crops such as maize and beans, which represent a small area of the basin (Souza et al. 2004; Santos et al. 2017). The Caatinga is a well-recognized ecological region that lies in the semiarid region hinterland of northeastern Brazil and that covers approximately 912,529 km² (Silva et al. 2017).

The climate in the Epitácio Pessoa reservoir catchment, according to De Medeiros et al. (2019) is equatorial tropical type (2d), hot semiarid, with a substantial temporal, spatial and interannual variability in rainfall; the dry season can last 8 months (June–January), and the wet season can last 4 months (February–May), as shown in Fig. 2. The historical rainfall in the basin indicates that the region presents an annual mean that ranges between 350

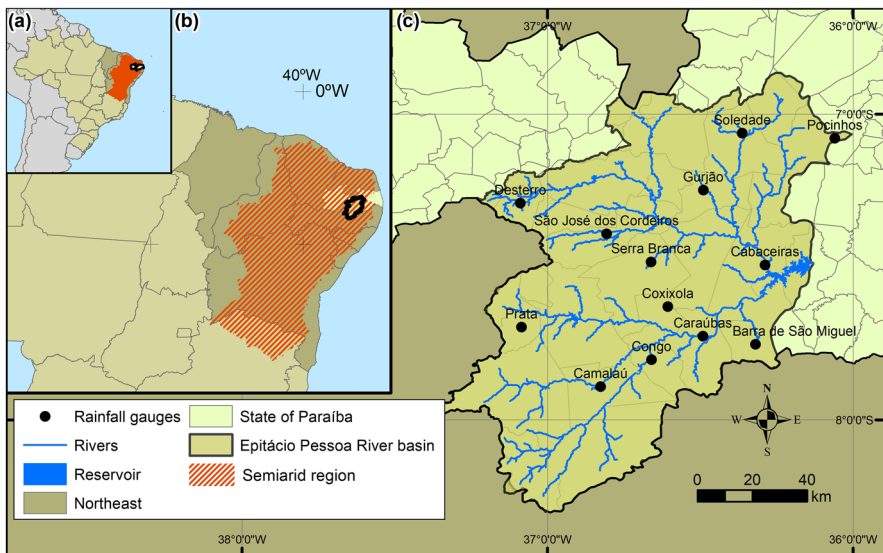


Fig. 1 Geographic locations of the rainfall gauges and Epitácio Pessoa reservoir catchment in northeastern Brazil and Paraíba State

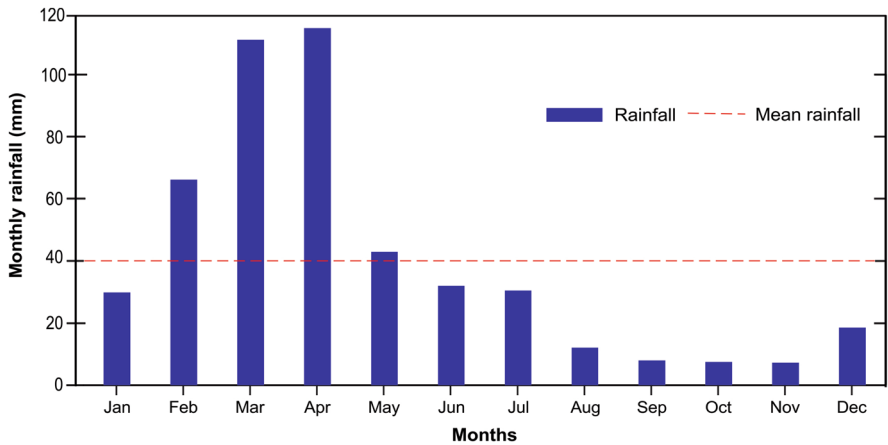


Fig. 2 Monthly mean rainfall hietograph in the Epiitácio Pessoa reservoir catchment (1963–1991)

and 600 mm/year, with a higher concentration in a period of 2–4 months (January–April), corresponding to 65% of the total annual rainfall (Srinivasan and Paiva 2009). Regarding the climatic influence in the region, the uniform action of the Atlantic masses provides a uniform temperature and rainfall gradient in the region. The higher rainfall rates in this area occur due to the intertropical convergence zone, mesoscale convective complexes, upper tropospheric cyclonic vortexes and instability lines (Dantas et al. 2020).

2.2 Rainfall data and drought severity/anomalies

For this study, monthly rainfall data for 13 rainfall gauges were obtained from the Paraíba State Water Management Executive Agency (Agência Executiva de Gestão de Águas do Estado da Paraíba—AESA) for the period from 1963 to 1991 (Table 1). The choice of these rainfall gauges was based on the amount of missing data during the studied period. The total percentage of missing rainfall data was 2.8%, ranging from 0 to 4% among the stations. Any missing data were filled into form a complete time series for the available period. To fill the missing data, the regional weighting method was used (Eq. 1). If X is the station with missing data and a , b and c are the surrounding stations, the weighted average record at the three surrounding rainfall gauges were used to determine the rainfall of X gauge as:

$$P_X = \frac{1}{3} \left(\frac{M_X}{M_a} P_a + \frac{M_X}{M_b} P_b + \frac{M_X}{M_c} P_c \right) \tag{1}$$

where P_X is the variable that will represent the corrected data, M_X is the arithmetic mean of the station with missing data, M_a , M_b and M_c are the arithmetic means of neighboring stations, and P_a , P_b and P_c are the data that were used to fill the missing values. These data are from the stations neighboring the station with missing data using linear distance (Table 2) from the same year.

The regional weighting method is generally used to fill in monthly to annual series, where the missing data of a station are filled using a weighting based on the data from

Table 1 Detailed description of the rainfall stations

Station	Code	Date period	Missing data (%)	Longitude (°)	Latitude (°)	Elevation (m)
Soledade	<i>P1</i>	1912–1993	3.19	−36.37	−7.07	560
Serra Branca	<i>P2</i>	1962–1994	5.47	−36.67	−7.48	450
São José dos Cord- eiros	<i>P3</i>	1962–1993	7.45	−36.82	−7.38	610
Pocinhos	<i>P4</i>	1923–1993	1.14	−36.07	−7.07	624
Gurjão	<i>P5</i>	1962–1993	4.02	−36.48	−7.27	480
Coxixola	<i>P6</i>	1962–1994	1.16	−36.62	−7.62	465
Congo	<i>P7</i>	1962–1994	8.95	−36.67	−7.80	500
Caraúbas	<i>P8</i>	1931–1993	5.48	−36.52	−7.72	460
Camalaú	<i>P9</i>	1962–1994	0.58	−36.87	−7.92	565
Cabaceiras	<i>P10</i>	1926–1994	0.84	−36.28	−7.60	390
Barra de São Miguel	<i>P11</i>	1962–1993	3.45	−36.33	−7.75	520
Prata	<i>P12</i>	1962–1994	6.32	−37.10	−7.68	600
Desterro	<i>P13</i>	1923–1993	4.30	−37.10	−7.28	590

Table 2 Matrix of distance between the rainfall stations (chosen stations in bold)

Stations	Distance (km)												
	<i>P1</i>	<i>P2</i>	<i>P3</i>	<i>P4</i>	<i>P5</i>	<i>P6</i>	<i>P7</i>	<i>P8</i>	<i>P9</i>	<i>P10</i>	<i>P11</i>	<i>P12</i>	<i>P13</i>
<i>P1</i>		56.8	60.8	33.2	25.6	66.8	87.6	73.8	109.1	59.7	75.7	105.9	84.5
<i>P2</i>	56.8		19.9	80.8	31.4	15.8	35.0	30.7	52.8	44.3	47.2	52.7	52.7
<i>P3</i>	60.8	19.9		90.0	39.0	34.0	49.0	49.6	59.3	63.6	67.0	45.6	33.2
<i>P4</i>	33.2	80.8	90.0		51.1	86.0	104.8	87.4	129.0	63.7	81.2	133.0	116.7
<i>P5</i>	25.6	31.4	39.0	51.1		41.4	62.4	49.9	83.4	43.0	56.0	82.2	68.1
<i>P6</i>	66.8	15.8	34.0	86.0	41.4		21.0	15.6	43.2	36.8	34.6	53.9	64.9
<i>P7</i>	87.6	35.0	49.0	104.8	62.4	21.0		18.9	25.6	47.8	37.2	49.5	74.5
<i>P8</i>	73.8	30.7	49.6	87.4	49.9	15.6	18.9		44.5	28.8	20.6	64.5	80.3
<i>P9</i>	109.1	52.8	59.3	129.0	83.4	43.2	25.6	44.5		73.3	61.7	36.5	74.6
<i>P10</i>	59.7	44.3	63.6	63.7	43.0	36.8	47.8	28.8	73.3		17.5	90.6	96.8
<i>P11</i>	75.7	47.2	67.0	81.2	56.0	34.6	37.2	20.6	61.7	17.5		84.9	99.2
<i>P12</i>	105.9	52.7	45.6	133.0	82.2	53.9	49.5	64.5	36.5	90.6	84.9		44.2
<i>P13</i>	84.5	52.7	33.2	116.7	68.1	64.9	74.5	80.3	74.6	96.8	99.2	44.2	

at least three neighboring stations, which should be from climatological regions similar to that of the station of interest and have a data series of at least 10 years (Santos et al. 2018).

The El Niño index was used to analyze the rainfall anomalies. Data from the Golden Gate Weather Services database (GGWS, 2019) were used to apply this index. The El Niño index indicates the intensity of the incidence of El Niño/La Niña phenomena from the mean sea surface temperature over three consecutive months in the El Niño 3.4 region in the Pacific Ocean. The range for each intensity class is as follows: (a) weak: 0.5–0.9, (b) moderate: 1.0–1.4, (c) strong: 1.5–1.9 and (d) very strong: ≥ 2.0 . The El

Niño index exhibits variation along its historical time series, which indicates high or low intensity of the reduction in rainfall in northeastern Brazil.

2.3 Analysis of rainfall trends

Statistical trend analysis methods assume the independence of the data to test the correlation between the data, which ensures the reliability of the results (Tomasella et al. 2018). Descriptive statistics techniques show the central position of the data (median) and whether there is symmetry or asymmetry in addition to showing the outliers, i.e., the values that diverge greatly from the other values in the series or are inconsistent with the series, which aid in understanding the data distribution.

Among the various methods of trend analysis, two nonparametric methods were chosen: Mann–Kendall (Mann 1945; Kendall 1975), suggested by the World Meteorological Organization, and Sen’s test (Sen 1968), which defines the magnitude of the trend. This integration of these two tests is used to detect significant trends and estimate the true slope of the trend. These methods have been widely used in hydrometeorological time series (Tabari et al. 2011; Gocic and Trajkovic 2013; Silva et al. 2015; Kisi et al. 2018). The Mann–Kendall method is applied in cases where the data values x_i of a time series can obey the following model:

$$x_i = f(t_i) + \varepsilon_i \tag{2}$$

where $f(t_i)$ is an increase or decrease in the monotonic function, and ε_i are the residuals assumed to have the same distribution with zero mean. It is then assumed that the variance in the distribution is constant. In this method, the null hypothesis (H_0) is tested, i.e., the observations x_i are ordered randomly against the hypothesis H_1 where there is a trend (Salmi et al. 2018). For the computation of this statistical test, both S statistics described in Santos et al. (2018) and the normal approximation (Z statistics) are exploited. Next, the variance S is calculated by the following equation:

$$\text{var}(S) = \frac{n(n - 1)(2n + 5) - \sum_{i=1}^p t_i(t_i - 1)(2t_i + 5)}{18} \tag{3}$$

where n is the number of data values, p represents the number of groups with repeated data, and t_i is the number of data values of the i th group. The values of S are used to calculate the test Z_S :

$$Z_s = \begin{cases} \frac{S-1}{\sqrt{\text{var}(S)}}, & S > 0 \\ 0, & S = 0 \\ \frac{S+1}{\sqrt{\text{var}(S)}}, & S < 0 \end{cases} \tag{4}$$

The presence of a trend is then evaluated by the value of Z_s . A positive value indicates an upward trend, and a negative value corresponds to a downward trend. If the null hypothesis is rejected, the level of significance (α) is calculated. Significance levels of 0.05 (*), 0.10 (**), and 0.15 (+) were used in this work.

The other nonparametric method used was Sen’s method. To estimate the slope of a trend using this method, the following equation was used:

$$f(t) = Q_t + B \quad (5)$$

where Q is the slope, and B is a constant. To estimate B , the n values of the difference $x_i - Q_{it}$ are calculated. The confidence intervals are then calculated at two different levels to assure the reliability of the test. Sen's method also makes it possible to identify whether or not there was a change in the trend and its magnitude, which is a technique widely used for this type of analysis (Santos et al. 2017; Kisi et al. 2018).

To obtain the slope estimate given in the above equation, it is necessary to calculate the slope of all the data pairs:

$$Q_i = \frac{x_j - x_k}{j - k} \text{ for } j > k \quad (6)$$

where x_j and x_k are the values of x in periods j and k , respectively. If there are n values x_j in the time series, then there are $N = n(n-1)/2$ estimates of slope Q_i . Thus, the slope estimated by the Sen's method is the median of these N values of Q_i . The N values of Q_i are classified from lowest to highest and the Sen's estimate is expressed as follows:

$$Q_{\text{med}} = \begin{cases} Q_{\lfloor \frac{(N+1)}{2} \rfloor}, & \text{if } N \text{ is an odd number} \\ \frac{1}{2} (Q_{\lfloor N/2 \rfloor} + Q_{\lfloor (N+1)/2 \rfloor}), & \text{if } N \text{ is an even number} \end{cases} \quad (7)$$

where Q_{med} reflects data trend, while its value indicates the steepness of the trend. To determine whether the median slope is significantly different from zero, the confidence interval of Q_{med} should be determined at a specific probability. The confidence interval about the time slope can be computed as follows:

$$C_\alpha = Z_{1-\alpha/2} \sqrt{\text{Var}(S)} \quad (8)$$

where $Z_{1-\alpha/2}$ is obtained from the standard normal distribution table. In this paper, the confidence interval was computed at three significance levels (0.05, 0.10 and 0.15). $M_1 = (n - C_\alpha)/2$ and $M_2 = (n + C_\alpha)/2$ were then computed. The lower and upper limits of the confidence interval, Q_{min} and Q_{max} , are the M_1 th largest and the $(M_2 + 1)$ th largest of the n -ordered slope estimates, respectively (Gilbert 1987). The slope Q_{med} is significantly different from zero if the two limits (Q_{min} and Q_{max}) have similar signs.

The Pettitt test uses the Mann–Whitney U test to find a single change point in the median of a series and returns a p value for the change point (Pettitt 1979). This test is robust to outliers and skewed distributions (Ryberg et al. 2020). In rare instances, the Pettitt test returns two change points because of ties in the data; in these instances, we used the first change point. The ranks of the $y_{1:n}(r_{1:n})$ are used to calculate the Pettitt statistic, which is based on the Mann–Whitney two-sample test:

$$P(k) = 2 \times \sum_i^i r_i - k(n + 1) \quad (9)$$

The probable change point U is located at the k value at which the absolute value of $P(k)$ is maximized.

$$U = \max_{1 \leq k < n} |P(k)| \quad (10)$$

The approximate probability for a two-sided test is calculated according to:

$$p\text{-value} = 2 \times \exp\left(\frac{-6U^2}{n^3 + n^2}\right) \tag{11}$$

2.4 Spatial analysis of rainfall

Spatial analysis is the process of manipulating spatial information to extract new information and meanings from the original data (Golla et al. 2019). The geostatistical interpolation method was used to determine the spatial distribution of rainfall in the catchment. The interpolation of data is of paramount importance to assess the spatial distribution of the data. Thus, rainfall and erosivity interpolation maps were generated, as were interpolation maps for the trend test results for each rainfall station for the studied period. To obtain the distribution of the rainfall data using spatial interpolation, the inverse distance-weighted (IDW) interpolator was used, which is expressed by:

$$f(x, y) = \frac{\sum_{j=1 \dots N} w(d_j) v_j}{\sum_{j=1 \dots N} w(d_j)} \tag{12}$$

where N is the number of data, v_j is the value of point j , d_j is the distance between the values of point j , and $w(d)$ is the weighting function. To obtain the value of $w(d)$, the following equation was used:

$$w(d) = \begin{cases} \frac{1}{d_{\min}^2}, & d \leq d_{\min} \\ \frac{1}{d^2}, & d_{\min} < d < d_{\max} \\ 0, & d > d_{\max} \end{cases} \tag{13}$$

where d_{\min} is the minimum distance, and d_{\max} is the maximum distance. The use of d_{\min} prevents the possibility of values with $d=0$, and the use of d_{\max} avoids the use of very distant points.

Interpolation using the IDW interpolator is based on the weighted distance of sample points, i.e., the surface interpolated by this method is created based on the use of a weighting coefficient that controls the spatial estimation of values for the sample points. The main advantage of the method is simplicity, leading to variable results for a wide variety of data, with no issues for results that exceed the range of significant values (Caruso and Quarta 1998). This method is based on spatial dependence, i.e., it assumes that the closer an individual sample point is to the other, the greater the correlation of this individual sample point with its neighbors. Thus, greater weight is assigned to the closer individual sample points than to those furthest from the point to be interpolated.

The model consists of multiplying the values observed by the inverse of their respective distances to the reference point for interpolation of the values (Eq. 12). This statistical model considers the existence of an effect of distance and of any other factor, which is represented by the letter “ p ”, i.e., the distance is raised to the power “ p ” so that different interpolated values can be obtained for the same distance. Rainfall spatialization using IDW was performed using ArcGIS 10.1® software.

2.5 Rainfall erosivity calculation

To calculate the rainfall erosivity, monthly rainfall data between January 1963 and December 1991 from 13 rainfall stations were used. The monthly rainfall erosivity of each station was determined using Eq. 14 (Da Silva 2004):

$$R_m = 42.307 \times (P_m^2/P_a) + 69.763 \quad (14)$$

where R_m is the rainfall erosivity factor ($\text{MJ mm ha}^{-1} \text{ h}^{-1} \text{ y}^{-1}$), P_m is the average monthly precipitation depth (mm), and P is the average annual precipitation (mm).

3 Results and discussion

3.1 Spatial–temporal variability of rainfall

Figure 3 presents the annual variability in rainfall at the studied stations. High variability is observed between 1963 and 1991 in the Epitácio Pessoa reservoir catchment, with an annual mean of 495.98 mm and a standard deviation of 237.50 mm. The results show modest temporal trends but strong and coherent spatial trends in the rainfall data from the Epitácio Pessoa reservoir catchment. Essentially, the findings agree with studies of other semiarid regions (Santos et al. 2019b; Ramos and Durán 2014), which highlighted intra- and interannual rainfall variability. The annual rainfall variations of approximately 350 mm are considered low, which caused an increase in the number of degraded areas during the study period, as reported by Silva et al. (2018). This expansion of the degradation area has been accelerated due to the severe droughts that recurred in this region in past decades, as shown by Tomasella et al. (2018), Awange et al. (2016) and Martins et al. (2018).

Figure 4 represents the rainfall variability at the analyzed stations. The results show that several years exhibited large water deficits or above-average rainfall throughout the region. The Prata station showed the highest annual rainfall values when compared to the other stations. It can be observed that the number of outliers is low (not exceeding two per series) and that the Prata station stands out as having the greatest data dispersion.

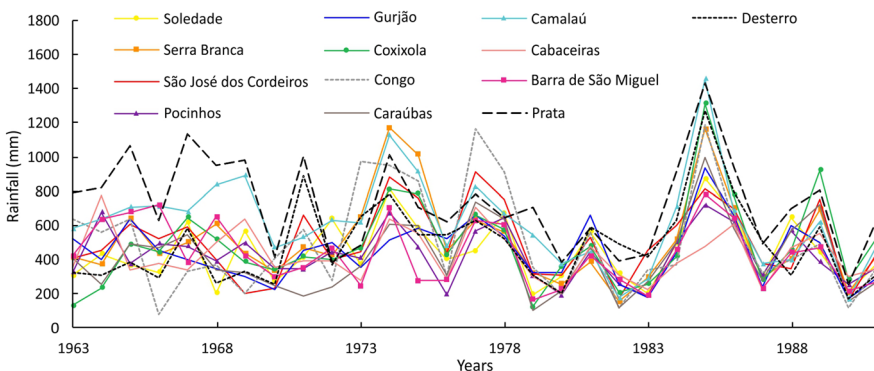


Fig. 3 Annual rainfall variability in the Epitácio Pessoa reservoir catchment between 1963 and 1991

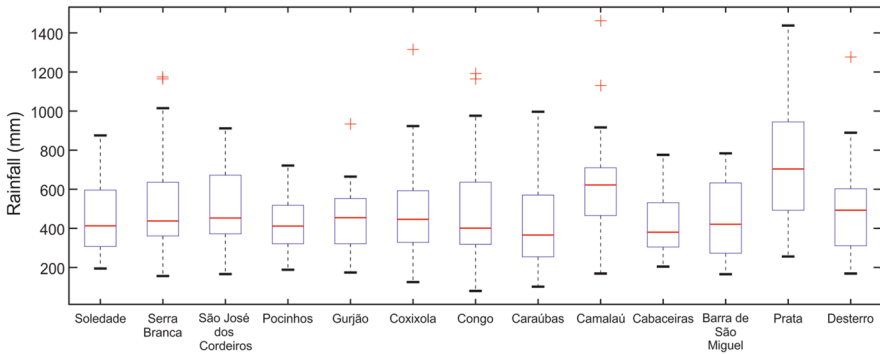


Fig. 4 Analysis of rainfall variability in the stations included in this study

Table 3 presents the mean values for each station and the variance (standard and mean deviations) of the data from the mean. The Congo station stands out due to its low standard deviations, which indicate that the values are closer to the mean, whereas the Camalaú and Prata stations presented the highest standard deviations. However, the Prata station indicated the highest standard deviation, unlike the other stations, which indicated relatively distant values. It should be noted that results for northeastern Brazil, especially the semiarid region, can be partly explained by variation in the general atmospheric circulation. Figure 5 shows the El Niño anomalies and the drought occurrence for northeastern Brazil between 1963 and 1991. Indeed, several studies have linked the decrease in rainfall to the El Niño-Southern Oscillation (ENSO), which influences the climate in South America and other parts of the world. In Brazil, this phenomenon affects parts of the northern, northeastern and extratropical areas of southern Brazil (Souza et al. 2018; da Silva et al. 2011). The climatic variability associated with the ENSO phases, especially rainfall anomalies, is quantifiable, and this information can be effectively used by crop managers to

Table 3 Descriptive analysis of the stations used in this study

Rainfall stations	Rainfall (mm)		
	Mean	SD	Mean deviation
Soledade	395.40	185.93	143.35
Serra Branca	495.08	257.48	157.88
São José dos Cordeiros	476.59	224.85	168.13
Pocinhos	383.14	160.62	137.11
Gurjão	442.65	174.68	194.53
Coxixola	470.04	257.94	190.25
Congo	446.07	55.86	171.27
Caraúbas	380.63	205.66	175.46
Camalaú	602.56	279.24	203.94
Cabaceiras	307.66	193.29	205.79
Barra de São Miguel	431.96	181.46	193.59
Prata	694.79	294.26	502.15
Desterro	383.18	244.45	148.50

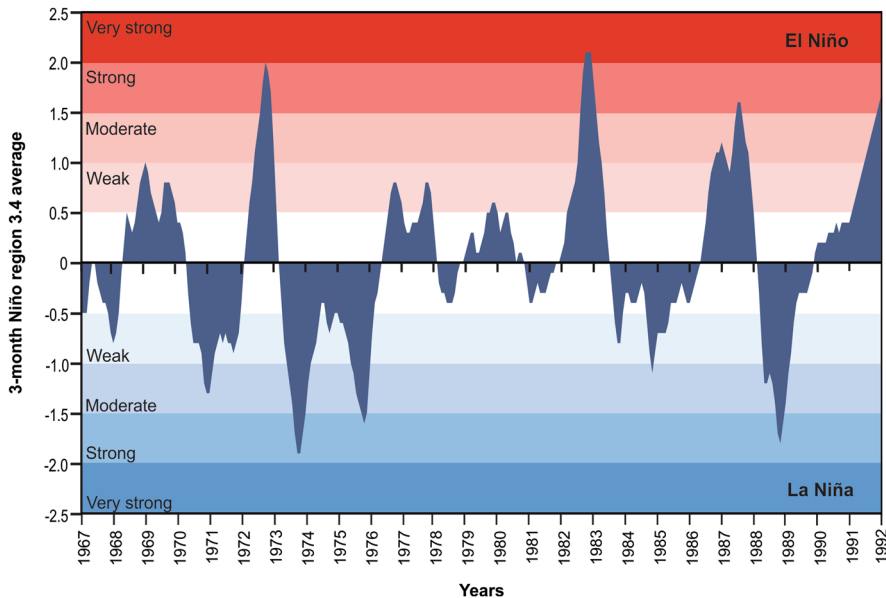


Fig. 5 Monthly values of the Oceanic Niño Index from 1963 to 1991. The El Niño Index shows warm (red) and cold (blue) phases of abnormal sea surface temperatures in the tropical Pacific Ocean

decrease the associated risk or to make better use of forthcoming favorable climatic conditions (Cunha et al. 2001). According to de Souza et al. (2005), the rainfall in northeastern Brazil is strongly modulated by the combined effects of sea surface temperature anomalies in the Pacific and Atlantic Oceans. Therefore, the connection between the Pacific and Atlantic Oceans has received particular interest, and some researchers have suggested that the ENSO-related atmospheric teleconnection plays an important role in Atlantic climatic variability (Ropelewski and Halpert 1987; Saravanan and Chang 2000).

Figure 6 shows the spatial distribution of rainfall in the Epitácio Pessoa reservoir catchment between 1963 and 1991. The highest and lowest rainfall values were identified in the southeastern and northeastern portions of the catchment, respectively. An analysis of the locations of the stations indicates that most of the closer stations tend to fall within the average rainfall range in the periods studied, except for the Cabaceiras (307.66 mm) and Prata (694.79 mm) stations, which are located far from the area of influence of the mean, and the Congo (446.07 mm) station, because it is located between the two stations.

3.2 Spatial–temporal analysis of annual rainfall trends

The Mann–Kendall and Sen’s methods were applied to analyze the rainfall trends. Table 4 shows the results of trends and significance for the analyzed data. The values that reject the null hypothesis are highlighted in this table, i.e., values that indicate a trend. The Soledade, Coxixola, Caraúbas and Desterro stations showed positive trends (upward). Using the results for the Sen slope, indications of decreasing trends were observed in the annual rainfall series for the Pocinhos, Gurjão, Serra Branca, São José dos Cordeiros, Congo, Cabaceiras, Camalaú and Prata rainfall stations. The Camalaú, Barra de São Miguel and Prata

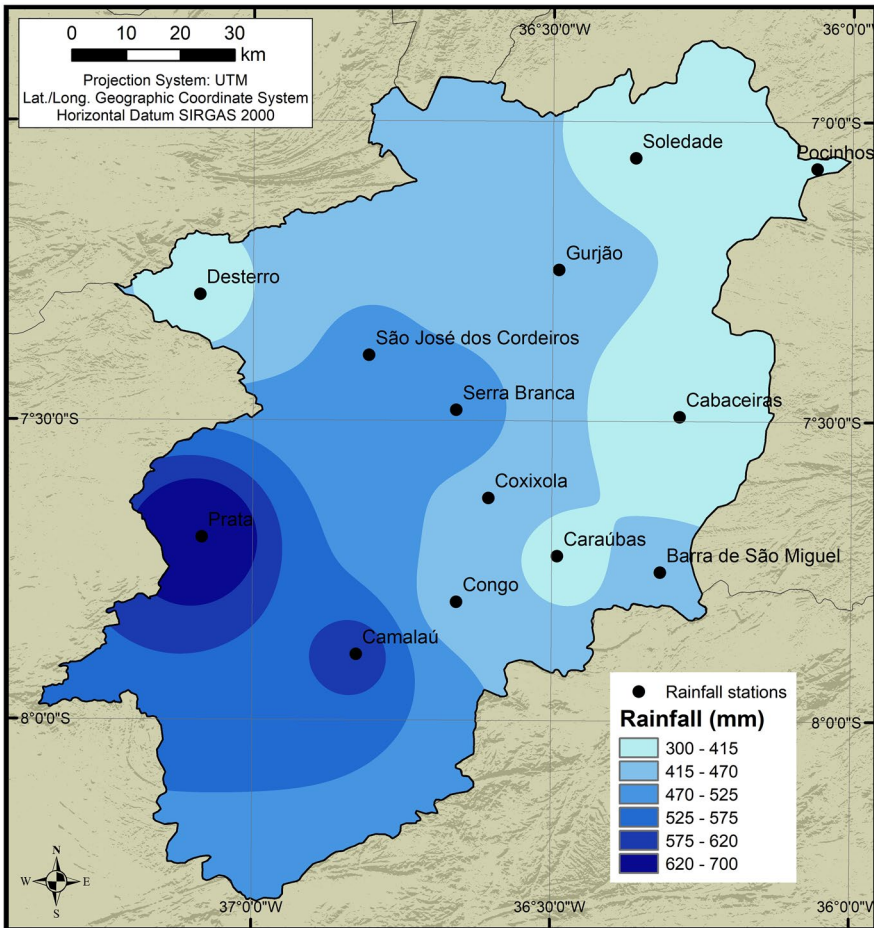


Fig. 6 Spatial distribution of the mean annual rainfall in the Epitácio Pessoa reservoir catchment

stations exhibited $H_0 = \text{Reject}$ (negative trend), with significance levels of 4.9%, 8.8% and 14.9%, respectively.

Negative trends (downward) with higher significance levels were recorded at the Camalaú, Barra de São Miguel and Prata stations, with -1.970 , -1.707 and -1.444 for the Z_S test and -11.300 , -7.208 and -9.808 for the Q test, respectively. At the other stations (Soledade, Serra Branca, São José dos Cordeiros, Pocinhos, Gurjão, Coixola, Congo, Caraúbas, Cabaceiras and Desterro), the null hypothesis was accepted and there was no evidence of a trend. It can be observed that the negative slope of trends calculated using the Q test ranged from -0.383 (São José dos Cordeiros station) to -11.300 (Camalaú station). Climate change plays a key role in the rainfall variability in the environments of the region, especially including the Caatinga biome, where it compromises water and energy security and the subsistence agriculture in the region. According to Marengo et al. (2018), the Caatinga biome presents multiple stressors on natural and human systems that are derived in part from significant changes in climate and are influenced by land use and cover change. This variability also influences the extreme events

Table 4 Results of the trend analysis based on the Mann–Kendall and Sen tests

Rainfall station	ID	Z_S	p value	Q	H_0
Soledade	P1	0.319	0.750	1.320	Accept
Serra Branca	P2	−0.694	0.488	−3.311	Accept
São José dos Cordeiros	P3	−0.131	0.896	−0.383	Accept
Pocinhos	P4	−0.619	0.536	−2.488	Accept
Gurjão	P5	−0.356	0.722	−1.050	Accept
Coxixola	P6	0.807	0.420	3.874	Accept
Congo	P7	−0.431	0.666	−2.464	Accept
Caraúbas	P8	0.244	0.807	1.199	Accept
Camalaú	P9	−1.970	0.049	−11.300	Reject*
Cabaceiras	P10	−0.807	0.420	−2.234	Accept
Barra de São Miguel	P11	−1.707	0.088	−7.208	Reject**
Prata	P12	−1.444	0.149	−9.808	Reject ⁺
Desterro	P13	0.600	0.536	2.859	Accept

Significance levels: *(0.05), **(0.10), +(0.15)

at various time scales, which affect social and natural systems and the high socioeconomic vulnerability of people in the semiarid region.

Figure 7a–m present the graphical representations of the Sen and Pettitt tests (magnitude and slope), which indicate the annual rainfall variability for each rainfall station. This absence of a significant trend in rainfall during the analyzed period is probably due to the substantial variability of rainfall that can be observed graphically (Fig. 7). The figures indicate that there is no change in the trend of the series studied, which are monotonic. In addition, they show the substantial variability in rainfall during the study period, especially for the Soledade (a), Coxixola (f), Caraúbas (h) and Desterro (m) stations, which also show evidence of trends in the Z_S test. The results of the Pettitt test are presented in Table 5, which indicates that the null hypothesis H_0 (homogeneous data) was accepted for all time series. These results are close to those obtained by Sena and Lucena (2013), Xavier et al. (2016) and Alves et al. (2017), who also analyzed rainfall trends in part of the studied basin.

This part of the paper is intended to describe regional variations in the spatial and temporal variability in the rainfall, i.e., to identify regions that exhibit similar rainfall variations. Figure 8a shows the spatial distribution of the results of the Z_S test for the Epitácio Pessoa reservoir catchment. The lowest values occur in the Prata, Barra de São Miguel and Camalaú stations, which are located in the central and southeastern regions of the basin. The intermediate values cover a large portion of the basin, including the Congo, Serra Branca, São José dos Cordeiros, Cabaceiras, Gurjão and Pocinhos stations. However, the highest values calculated using the Z_S test were identified more precisely in the central and northern regions of the catchment and refer to the Soledade, Coxixola, Caraúbas and Desterro stations. This spatial consistency can be explained by the substantial inhomogeneity of the rainfall regime in the catchment. Figure 8b shows the spatial distribution of the data resulting from Sen's method, which shows the spatial similarity of the data between the two methods. The highest values were observed at stations in the central, northern and eastern portions of the catchment. These results can be explained by the substantial variability of the rainfall index in the studied region.

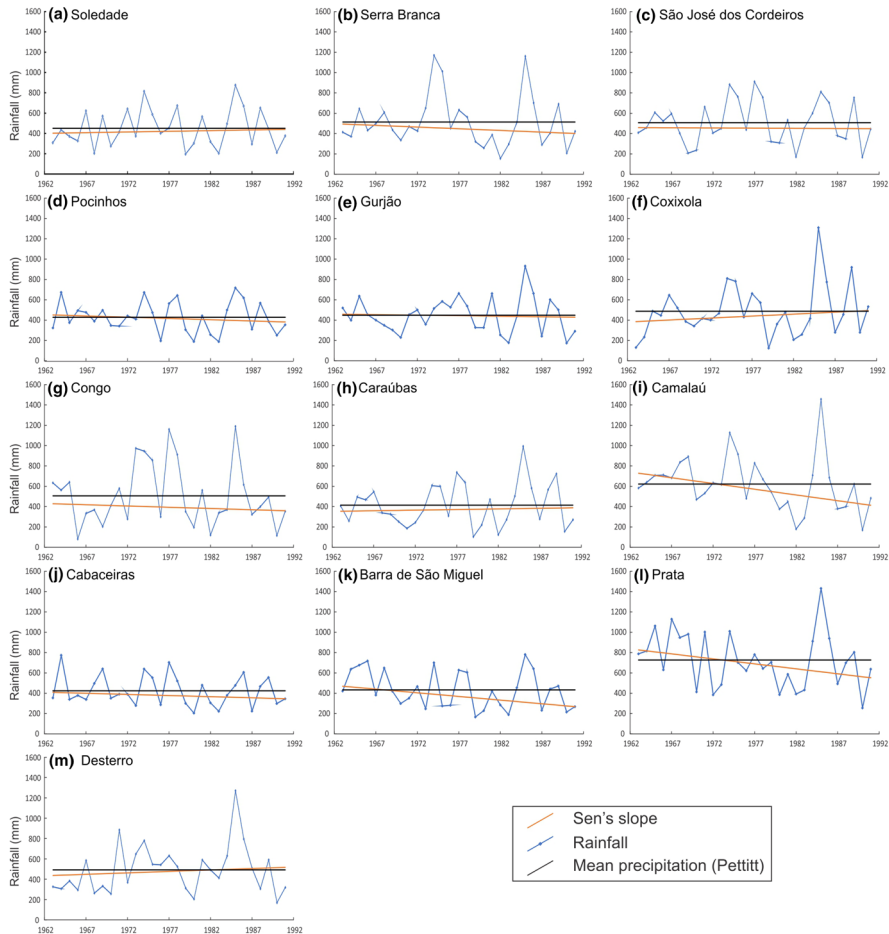


Fig. 7 Annual rainfall variation using the Sen and Pettitt tests for the following stations: **a** Soledade, **b** Serra Branca, **c** São José dos Cordeiros, **d** Pocinhos, **e** Gurjão, **f** Coxixola, **g** Congo, **h** Caraúbas, **i** Camalaú, **j** Cabaceiras, **k** Barra de São Miguel, **l** Prata and **m** Desterro

3.3 Spatiotemporal representativity of the rainfall erosivity dataset

Figure 9 shows the spatial distribution of the average rainfall erosivity for the wet and dry seasons, the average monthly erosivity and annual trends of rainfall erosivity. The results show that the erosivity values were within the range of 480–1200 MJ mm ha⁻¹ h⁻¹ yr⁻¹ for the wet season (Fig. 9a) and 93–164 MJ mm ha⁻¹ h⁻¹ yr⁻¹ for the dry season (Fig. 9b), i.e., a difference greater than 500% between the two seasons. In comparison, the erosivity values for the wet season increased from east to west and from west to east in the dry season. The results from this study show that erosivity in the region was low because of the intensity and amount of rainfall; however, many extreme events occur in the region that cause serious impacts to the environment such as land degradation. In the wet season, the average annual erosivity density was highest around the Prata rainfall station along the state border and at higher elevations. Erosivity density varied not only among the stations

Table 5 Results for the Pettitt test

Rainfall gauges	Station code	U	t	p value	Hypothesis	
					H_0	Risk
Soledade	P1	46	1970	0.262	Accepted	26.22
Serra Branca	P2	90	1978	0.358	Accepted	35.82
São José dos Cordeiros	P3	52	1978	0.461	Accepted	46.10
Pocinhos	P4	58	1978	0.693	Accepted	69.32
Gurjão	P5	46	1989	0.257	Accepted	25.68
Coxixola	P6	54	1984	0.532	Accepted	53.22
Congo	P7	62	1978	0.835	Accepted	83.54
Caraúbas	P8	50	1972	0.385	Accepted	38.48
Camalaú	P9	118	1978	0.070	Accepted	7.02
Cabaceiras	P10	72	1978	0.804	Accepted	80.44
Barra de São Miguel	P11	82	1968	0.526	Accepted	52.56
Prata	P12	92	1969	0.323	Accepted	32.30
Desterro	P13	96	1970	0.263	Accepted	26.28

U change point, t year when the mean rainfall changed, H_0 homogeneous data, and $risk$ risk to reject H_0

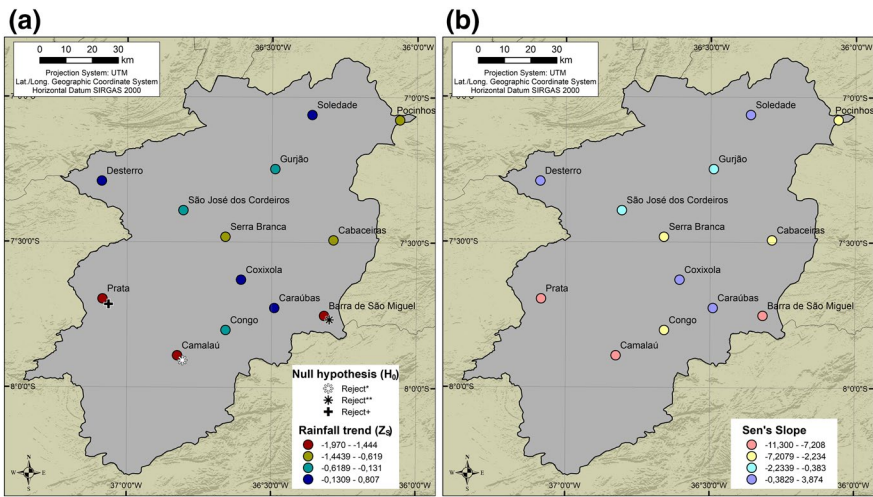


Fig. 8 **a** Spatial distribution of the results obtained using the Mann–Kendall method for the rainfall stations used in this study and **b** spatialization of the results obtained by Sen’s method for the rainfall stations used in this study

but also between months because these conditions change in the dry season and because the area around the Pocinhos rainfall station, located in the northeastern zone (as opposed to the Prata rainfall gauge, which is located in the southwestern zone), is the area with the highest erosivity values ($164 \text{ MJ mm ha}^{-1} \text{ h}^{-1} \text{ yr}^{-1}$).

Figure 9c shows that the highest erosivity values occurred between February and April and that there is a greater than 70% concentration of erosivity in that period. These results suggest that there must be preventive measures during this period to protect the soil from

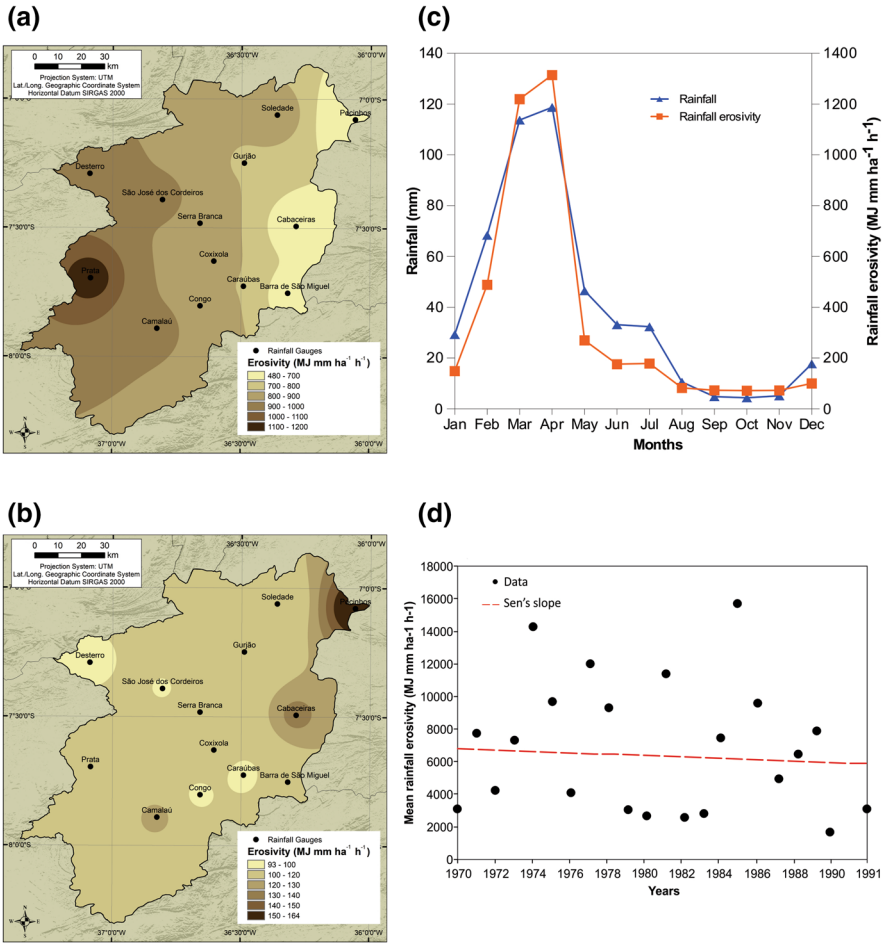


Fig. 9 **a** Spatial distribution of mean rainfall erosivity for the wet season, **b** spatial distribution of mean rainfall erosivity for dry season, **c** mean monthly erosivity and **d** mean annual erosivity for the study area

erosion and avoid soil degradation (Fig. 9c). The results presented in this study regarding erosivity trends indicate that the trend is positive for four rainfall stations and is negative for nine stations, while the results showed no trends for the catchment study area in its entirety (Fig. 9d).

4 Conclusions

In this study, the Mann–Kendall trend and Sen’s slope methods were used to investigate the temporal–spatial trends, rainfall variability and erosivity index for 13 rainfall stations in which each station provided data for over a 30-year period in the Epitácio Pessoa reservoir catchment. This work confirms the large spatial variability of trends in rainfall. Based on the results obtained, positive and negative trends were identified. The low spatial coherence of the trends found in the time series is consistent with the mixed pattern of positive

and negative changes at the global scale, especially those identified in northeastern Brazil. The Mann–Kendall and Sen's tests showed significant (downward) trends at the 15% significance level at the Camalaú, Barra de São Miguel and Prata stations. Exceptions were recorded in the other stations, whose trend tests were not statistically significant and in which changes in the time series occurred in different periods. The most noteworthy results observed were that (a) most of the calculated trend slopes are statistically nonsignificant and less than 25% of them are statistically significant at $\alpha=0.15$ and (b) the distribution of negative and positive trend slopes in the catchment is extremely irregular. The nonparametric Mann–Kendall test used in this study allowed a more comprehensive analysis of the climatic trends of rainfall time series, providing important information to help support more conclusive conclusions about the anomalies observed in some climatic parameters.

Erosivity is the core driver of most soil erosion processes through its influence on particle detachment and overland flow in the region. There were no trends of erosivity and reduced rainfall in the eastern portion of the study area for the wet season, with a stronger core at the Camalaú station, while such trends occurred in the dry season in the western portion. These results need to be combined with information on land use in the catchment to identify possible causes of this variation. For example, if other methods were used to fill the gaps of missing data or rainfall data from other sources were used, the results may be affected.

Acknowledgements This study was financed in part by the Brazilian Federal Agency for the Support and Evaluation of Graduate Education (Coordenação de Aperfeiçoamento de Pessoal de Nível Superior - CAPES) – Fund Code 001, the National Council for Scientific and Technological Development, Brazil – CNPq (Grant Nos. 304213/2017-9 and 304540/2017-0) and Federal University of Paraíba.

Author contributions R.M.S., C.A.G.S. and J.F.C.B.C.S. designed research; R.M.S., C.A.G.S., J.F.C.B.C.S., A.M.S. and R.M.B.N. conducted review and editing; R.M.S. and C.A.G.S. provided funding acquisition, project administration and resources; and R.M.S., C.A.G.S., J.F.C.B.C.S. and R.M.B.N. wrote the paper.

Compliance with ethical standards

Conflict of interest The author(s) declare no competing interests.

Open Access This article is licensed under a Creative Commons Attribution 4.0 International License, which permits use, sharing, adaptation, distribution and reproduction in any medium or format, as long as you give appropriate credit to the original author(s) and the source, provide a link to the Creative Commons licence, and indicate if changes were made. The images or other third party material in this article are included in the article's Creative Commons licence, unless indicated otherwise in a credit line to the material. If material is not included in the article's Creative Commons licence and your intended use is not permitted by statutory regulation or exceeds the permitted use, you will need to obtain permission directly from the copyright holder. To view a copy of this licence, visit <http://creativecommons.org/licenses/by/4.0/>.

References

- Alvalá RCS, Cunha APMA, Brito SSB, Seluchi ME, Marengo JA, Moraes OLL, Carvalho MA (2017) Drought monitoring in the Brazilian Semiarid region. *Ann Braz Acad Sci* 91(Suppl. 1):e20170209. <https://doi.org/10.1590/0001-3765201720170209>
- Alves TLB, de Azevedo PV, Costa dos Santos CA (2017) Influence of climate variability on land degradation (desertification) in the watershed of the upper Paraíba River. *Theor Appl Climatol* 127:741–751. <https://doi.org/10.1007/s00704-015-1661-1>

- Andreoli RV, Kayano MT (2007) A importância relativa do atlântico tropical sul e pacífico leste na variabilidade de precipitação do Nordeste do Brasil. *Rev Bras Meteorol* 22:63–74. <https://doi.org/10.1590/S0102-77862007000100007>
- Awange JL, Mpelasoka F, Goncalves RM (2016) When every drop counts: analysis of droughts in Brazil for the 1901–2013 period. *Sci Total Environ* 566–567:1472–1488. <https://doi.org/10.1016/j.scitotenv.2016.06.031>
- Barbosa HA, Kumar TVL (2016) Influence of rainfall variability on the vegetation dynamics over North-eastern Brazil. *J Arid Environ* 124:377–387. <https://doi.org/10.1016/j.jaridenv.2015.08.015>
- Brito SSB, Cunha APMA, Cunningham CC, Alvalá RC, Marengo JA, Carvalho MA (2017) Frequency, duration and severity of drought in the Semiarid Northeast Brazil region. *Int J Climatol* 38:517–529. <https://doi.org/10.1002/joc.5225>
- Caruso C, Quarta F (1998) Interpolation methods comparison. *Comput Math Appl* 35:109–126. [https://doi.org/10.1016/S0898-1221\(98\)00101-1](https://doi.org/10.1016/S0898-1221(98)00101-1)
- Costa RL, Baptista GMM, Gomes HB, Silva FDS, Rocha Júnior RL, Salvador MA, Herdies DL (2020) Analysis of climate extremes indices over northeast Brazil from 1961 to 2014. *Weather Clim Extrem* 28:100254. <https://doi.org/10.1016/j.wace.2020.100254>
- Croitoru A-E, Chiotoroiu B-C, Todorova VI, Torica V (2013) Changes in precipitation extremes on the Black Sea Western Coast. *Glob Planet Change* 102:10–19. <https://doi.org/10.1016/j.gloplacha.2013.01.004>
- Cunha GR, Dalmago GA, Estefanel V (2001) El Niño-southern oscillation influences on wheat crop in Brazil. In: Bedö Z, Láng L (eds) *Wheat in a global environment. Developments in plant breeding*, vol 9. Springer, Dordrecht, pp 445–450
- Da Silva AM (2004) Rainfall erosivity map for Brazil. *CATENA* 57(3):251–259. <https://doi.org/10.1016/j.catena.2003.11.006>
- da Silva GAM, Drumond A, Ambrizzi T (2011) The impact of El Niño on South American summer climate during different phases of the Pacific Decadal Oscillation. *Theor Appl Climatol* 106:307–319. <https://doi.org/10.1007/s00704-011-0427-7>
- da Silva VPR, Belo Filho AF, Almeida RSR, de Holanda RM, Campos JHBC (2016) Shannon information entropy for assessing space–time variability of rainfall and streamflow in semiarid region. *Sci Total Environ* 544:330–338. <https://doi.org/10.1016/j.scitotenv.2015.11.082>
- Dantas JC, Silva RM, Santos CAG (2020) Drought impacts, social organization and public policies in northeastern Brazil: a case study of the Upper Paraíba River basin. *Environ Monit Assess* 192:765–785. <https://doi.org/10.1007/s10661-020-8219-0>
- de Medeiros IC, Silva JFCBC, Silva RM, Santos CAG (2019) Run-off-erosion modelling and water balance in the Epitácio Pessoa Dam river basin, Paraíba State in Brazil. *Int J Environ Sci Technol* 15:1–14. <https://doi.org/10.1007/s13762-018-1940-3>
- de Souza EB, Kayano MT, Ambrizzi T (2005) Intraseasonal and submonthly variability over the Eastern Amazon and Northeast Brazil during the autumn rainy season. *Theor Appl Climatol* 81:177–191. <https://doi.org/10.1007/s00704-004-0081-4>
- Fernandez JPR, Franchito SH, Rao VB (2019) Future changes in the aridity of South America from regional climate model projections. *Pure Appl Geophys* 176(6):2719–2728. <https://doi.org/10.1007/s00024-019-02108-4>
- Galvão CO, Nobre P, Braga ACFM, Oliveira KF, Silva RM, Silva SR, Santos CAG, Gomes Filho MF, Lacerda F, Moncunill D (2005) Climatic predictability, hydrology and water resources over Nordeste Brazil. *IAHS Publ* 295:211–220
- Gilbert RO (1987) *Statistical methods for environmental pollution monitoring*. Wiley, New York
- Gocic M, Trajkovic S (2013) Analysis of changes in meteorological variables using Mann–Kendall and Sen’s slope estimator statistical tests in Serbia. *Glob Planet Change* 100:172–182. <https://doi.org/10.1016/j.gloplacha.2012.10.014>
- Golla V, Arveti N, Etikala B, Sreedhar Y, Narasimhlu K, Harish P (2019) Data sets on spatial analysis of hydro geochemistry of Gudur area, SPSR Nellore district by using inverse distance weighted method in Arc GIS 10.1. *Data Br* 22:1003–1011. <https://doi.org/10.1016/j.dib.2019.01.030>
- Gomes ACC, Bernardo N, Alcântara E (2017) Accessing the southeastern Brazil 2014 drought severity on the vegetation health by satellite image. *Nat Hazards* 89:1401–1420. <https://doi.org/10.1007/s11069-017-3029-6>
- Guo E, Zhang J, Wang Y, Quan L, Zhang R, Zhang F, Zhou M (2019) Spatiotemporal variations of extreme climate events in Northeast China during 1960–2014. *Ecol Indic* 96:669–683. <https://doi.org/10.1016/j.ecolind.2018.09.034>

- Hamlaoui-Moulai L, Mesbah M, Souag-Gamane D, Medjerab A (2013) Detecting hydro-climatic change using spatiotemporal analysis of rainfall time series in Western Algeria. *Nat Hazards* 65:1293–1311. <https://doi.org/10.1007/s11069-012-0411-2>
- Kendall MG (1975) Rank correlation methods. Griffin, London
- Kisi Ö, Santos CAG, da Silva RM, Zounemat-Kermani M (2018) Trend analysis of monthly streamflows using Sen's innovative trend method. *Geofizika* 35:53–68. <https://doi.org/10.15233/gfz.2018.35.3>
- Li D, Lu XX, Yang X, Chen L, Lin L (2018) Sediment load responses to climate variation and cascade reservoirs in the Yangtze River: a case study of the Jinsha River. *Geomorphology* 322:41–52. <https://doi.org/10.1016/j.geomorph.2018.08.038>
- Mann HB (1945) Nonparametric tests against trend. *Econometrica* 13:245–259
- Marçal NA, da Silva RM, Santos CAG, dos Santos JS (2019) Analysis of the environmental thermal comfort conditions in public squares in the semiarid region of northeastern Brazil. *Build Environ* 152:145–159. <https://doi.org/10.1016/j.buildenv.2019.02.016>
- Marengo JA (2008) Água e mudanças climáticas. *Estudos Avançados* 22:83–96. <https://doi.org/10.1590/S0103-40142008010200001>
- Marengo JA, Bernasconi M (2015) Regional differences in aridity/drought conditions over Northeast Brazil: present state and future projections. *Clim Change* 129:103–115. <https://doi.org/10.1007/s10584-014-1310-1>
- Marengo JA, Alves LM, Alvalá RCS, Cunha AP, Brito S, Moraes OLL (2018) Climatic characteristics of the 2010–2016 drought in the semiarid Northeast Brazil region. *Ann Braz Acad Sci* 90:1973–1985. <https://doi.org/10.1590/0001-3765201720170206>
- Martins MA, Tomasella J, Rodriguez DA, Alvalá RCS, Giarolla A, Garofolo LL, Siqueira Júnior JL, Paolicchi LTLC, Pinto GLN (2018) Improving drought management in the Brazilian semiarid through crop forecasting. *Agric Syst* 160:21–30. <https://doi.org/10.1016/j.agry.2017.11.002>
- Moghim S (2018) Impact of climate variation on hydrometeorology in Iran. *Glob Planet Change* 170:93–105. <https://doi.org/10.1016/j.gloplacha.2018.08.013>
- Morbidegli R, Saltalippi C, Flammini A, Corradini C, Wilkinson SM, Fowler HJ (2018) Influence of temporal data aggregation on trend estimation for intense rainfall. *Adv Water Resour* 122:304–316. <https://doi.org/10.1016/j.advwatres.2018.10.027>
- Mullick MRA, Nur RM, Alam MJ, Islam KMA (2019) Observed trends in temperature and rainfall in Bangladesh using pre-whitening approach. *Glob Planet Change* 172:104–113. <https://doi.org/10.1016/j.gloplacha.2018.10.001>
- Pettitt AN (1979) A non-parametric approach to the change-point problem. *J R Stat Soc* 28(2):126–135. <https://doi.org/10.2307/2346729>
- Pilz T, Delgado JM, Voss S, Vormoor K, Francke T, Costa AC, Martins E, Bronstert A (2018) Seasonal drought prediction for semiarid northeast Brazil: about the added value of a process-based hydrological model. *Hydrol Earth Syst Sci Discuss*. <https://doi.org/10.5194/hess-23-1951-2019>
- Ramos MC, Durán B (2014) Assessment of rainfall erosivity and its spatial and temporal variabilities: case study of the Penedés area (NE Spain). *CATENA* 123:135–147. <https://doi.org/10.1016/j.catena.2014.07.015>
- Ropelewski CF, Halpert MS (1987) Global and regional scale precipitation associated with El Niño/southern oscillation. *Mon Weather Rev* 115:1606–1626. [https://doi.org/10.1175/1520-0493\(1987\)115%3c1606:GARSPP%3e2.0.CO;2](https://doi.org/10.1175/1520-0493(1987)115%3c1606:GARSPP%3e2.0.CO;2)
- Rutebuka J, De Taeye S, Kagabo D, Verdoodt A (2020) Calibration and validation of rainfall erosivity estimators for application in Rwanda. *CATENA* 190:104538. <https://doi.org/10.1016/j.catena.2020.104538>
- Ryberg KR, Hodgkins GA, Dudley RW (2020) Change points in annual peak streamflows: method comparisons and historical change points in the United States. *J Hydrol* 583:124307. <https://doi.org/10.1016/j.jhydrol.2019.124307>
- Salmi T, Määttä A, Anttila P, Ruoho-Airola T, Amnell T (2018) Detecting trends of annual values of atmospheric pollutants by the Mann–Kendall test and Sen's slope estimates: the excel template application. Finnish Meteorological Institute, 2002. <http://en.ilmatieteenlaitos.fi/makesens>. Accessed 15 Mar 2018
- Santos CAG, Silva RM, Silva AM, Brasil Neto RM (2017) Estimation of evapotranspiration for different land covers in a Brazilian semi-arid region: a case study of the Brígida River basin, Brazil. *J S Am Earth Sci* 74:54–66. <https://doi.org/10.1016/j.jsames.2017.01.002>
- Santos CAG, Kisi Ö, da Silva RM, Zounemat-Kermani M (2018) Wavelet-based variability on streamflow at 40-year timescale in the Black Sea region of Turkey. *Arab J Geosci* 11:169–182. <https://doi.org/10.1007/s12517-018-3514-6>

- Santos CAG, Brasil Neto RM, da Silva RM, Costa SGF (2019a) Cluster analysis applied to spatiotemporal variability of monthly precipitation over Paraíba state using tropical rainfall measuring mission (TRMM) data. *Remote Sens* 11(6):637. <https://doi.org/10.3390/rs11060637>
- Santos CAG, Brasil Neto RM, Santos DC, Silva RM (2019b) Innovative approach for geospatial drought severity classification: a case study of Paraíba state, Brazil. *Stoch Environ Res Risk Assess* 33:545–562. <https://doi.org/10.1007/s00477-018-1619-9>
- Saravanan R, Chang P (2000) Interaction between tropical Atlantic variability and El Niño-Southern oscillation. *J Clim* 13:2177–2194. [https://doi.org/10.1175/1520-0442\(2000\)013%3c2177:IBTAV-A%3e2.0.CO;2](https://doi.org/10.1175/1520-0442(2000)013%3c2177:IBTAV-A%3e2.0.CO;2)
- Sen PK (1968) Estimates of the regression coefficient based on Kendall's tau. *J Am Stat Assoc* 63:1379–1389
- Sena JPO, Lucena DB (2013) Identification of precipitation trend in the microregion of cariri paraibano. *Revista Brasileira de Geografia Física* v.6, n.5 2013:1400–1416. <https://doi.org/10.26848/rbgf.v6.5.p1400-1416> (in portuguese)
- Silva RM, Santos CAG, Moreira M, Corte-Real J, Silva VCL, Medeiros IC (2015) Rainfall and river flow trends using Mann-Kendall and Sen slope estimator statistical tests in the Cobres River basin. *Nat Hazards* 77:1205–1221. <https://doi.org/10.1007/s11069-015-1644-7>
- Silva JMC, Barbosa LCF, Leal IR, Tabarelli M (2017) The caatinga: understanding the challenges. In: Silva JMC, Leal IR, Tabarelli M (eds) *Caatinga*. Springer, Cham. https://doi.org/10.1007/978-3-319-68339-3_1
- Silva RM, Santos CAG, Maranhão KUA, Silva AM, Lima VRP (2018) Geospatial assessment of eco-environmental changes in desertification area of the Brazilian semi-arid region. *Earth Sci Res J* 22:175–186. <https://doi.org/10.15446/esrj.v22n3.69904>
- Souza BI, Silans AMBP, Santos JB (2004) Contribuição ao estudo da desertificação na Bacia do Taperoá. *Rev Bras Eng Agríc Ambient* 8:292–298. <https://doi.org/10.1590/S1415-43662004000200019>
- Souza TCO, Delgado RC, Magistrali IC, dos Santos GL, de Carvalho DC, Teodoro PE, da Silva Júnior CA, Caúla RH (2018) Spectral trend of vegetation with rainfall in events of El Niño-Southern Oscillation for Atlantic Forest biome, Brazil. *Environ Monit Assess* 190:688. <https://doi.org/10.1007/s10661-018-7060-1>
- Srinivasan VS, Paiva FML (2009) Regional validity of the parameters of a distributed runoff-erosion model in the semi-arid region of Brazil. *Sci China Ser E Technol Sci* 52:3348–3356. <https://doi.org/10.1007/s11431-009-0345-4>
- Tabari H, Shifteh Somee B, Rezaeian Zadeh M (2011) Testing for long-term trends in climatic variables in Iran. *Atmos Res* 100(1):132–140. <https://doi.org/10.1016/j.atmosres.2011.01.005>
- Thomson P, Bradley D, Katilu A, Katuva J, Lanzoni M, Koehler J, Hope R (2019) Rainfall and groundwater use in rural Kenya. *Sci Total Environ* 649:722–730. <https://doi.org/10.1016/j.scitotenv.2018.08.330>
- Tomasella J, Vieira RMSP, Barbosa AA, Rodriguez DA, Santana MO, Sestini MF (2018) Desertification trends in the Northeast of Brazil over the period 2000–2016. *Int J Appl Earth Obs Geoinf* 73:197–206. <https://doi.org/10.1016/j.jag.2018.06.012>
- Xavier APC, Silva RM, Silva AM, Santos CAG (2016) Mapping soil erosion vulnerability using remote sensing and GIS: a case study of Mamuaba watershed, Paraíba State. *Revista Brasileira de Cartografia* 68(9):1677–1688

Publisher's Note Springer Nature remains neutral with regard to jurisdictional claims in published maps and institutional affiliations.